

AD-A034 395

NAVAL UNDERWATER SYSTEMS CENTER NEW LONDON CONN NEW --ETC F/G 9/2
FORTRAN PROGRAM FOR LINEAR PREDICTIVE SPECTRAL ANALYSIS OF A CO--ETC(U)
DEC 76 A H NUTTALL
NUSC-TR-5505

UNCLASSIFIED

NL

| OF |
AD
A034395



END

DATE
FILMED
2-77

ADA 034395

NUSC Technical Report 5505

NUSC Technical Report 5505

12



Fortran Program for Linear Predictive Spectral Analysis of a Complex Univariate Process

Albert H. Nuttall
Special Projects Department

3 December 1976

COPY AVAILABLE TO DDC DOES NOT
PERMIT FULLY LEGIBLE PRODUCTION

Copy available to DDC does not
permit fully legible reproduction

DDC
REF ID: A61112
JAN 14 1977
REGISTRY

NUSC

NAVAL UNDERWATER SYSTEMS CENTER
Newport, Rhode Island • New London, Connecticut

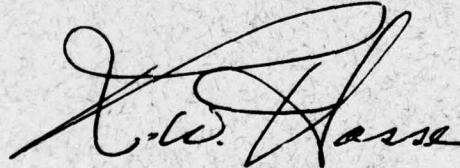
Approved for public release; distribution unlimited.

PREFACE

This research was conducted under NUSC Project No. A-752-05, "Applications of Statistical Communication Theory to Acoustic Signal Processing," Principal Investigator, Dr. A. H. Nuttall (Code 313), Navy Project No. ZR 000 01, Program Manager, T. A. Kleback (MAT 03521), Naval Material Command.

The Technical Reviewer for this report was H. Freese (Code 3103).

REVIEWED AND APPROVED: 3 December 1976

A handwritten signature in cursive script, appearing to read "R. W. Hasse".

R. W. Hasse

Head: Special Projects Department

The author of this report is located at the New London
Laboratory, Naval Underwater Systems Center,
New London, Connecticut 06320.

TABLE OF CONTENTS

	Page
LIST OF ILLUSTRATIONS	ii
LIST OF SYMBOLS	iii
1. INTRODUCTION	1
2. USE OF PROGRAM FOR SPECTRAL ANALYSIS	2
3. ESTIMATION OF CROSS-SPECTRUM OF TWO REAL PROCESSES	7
4. A LIMITATION OF COMPLEX PREDICTIVE FILTER	11
5. DISCUSSION	17
APPENDIX A--FORTRAN PROGRAM FOR SPECTRAL ANALYSIS	A-1
APPENDIX B--PROPERTY OF AUTOREGRESSIVE MODEL	B-1
APPENDIX C--NONANALYTIC WHITE NOISE EXCITATION	C-1
APPENDIX D--A METHOD OF GENERATING ANALYTIC PROCESSES	D-1
APPENDIX E--CAPABILITY OF A MORE GENERAL PREDICTION MODEL	E-1
LIST OF REFERENCES	R-1

ACCESSION for	
NWS	White Section <input checked="" type="checkbox"/>
DDC	Def. Section <input type="checkbox"/>
UNANNOUNCED	
JUSTIFICATION	
BY	
DISTRIBUTION/AVAILABILITY NOTES	
MIN.	AVAIL. BY/IN SPECIAL
A	

LIST OF ILLUSTRATIONS

Figure		Page
1	Spectrum of Surface-Bottom Forward Scatter	5
2	Spectrum of Direct Path	6

LIST OF SYMBOLS

N	Number of complex data points
P _{MAX}	Maximum order of filter considered
J	Size of FFT for spectral estimate
P _{BEST}	Best order of filter
Δ	Sampling interval in time
t	Time
u(t), v(t)	Real processes
Asterisk	Conjugate
α, β	Complex constants
x(t)	Complex process
$R_{xx}(\tau)$	Correlation of x(t) at delay τ
$R_{uv}(\tau)$	Crosscorrelation of u(t) and v(t)
f	Frequency
$G_{xx}(f)$	Auto-Spectrum of x(t)
R(f), I(f)	Real and imaginary parts of $G_{uv}(f)$
Re z	Real part of z
Im z	Imaginary part of z
\hat{x}_k	Estimate of x_k
a_n	n-th predictive coefficient
p	Order of predictive filter
\tilde{x}_k	More general estimate of x_k ; (19)
g_n, h_n	Complex filter coefficients

LIST OF SYMBOLS (Cont'd)

w_k	Excitation process in autoregression
δ_{on}	Kronecker delta: = 1 if $n = 0$, = 0 otherwise
Overbar	Ensemble average
R_n, \bar{R}_n	Correlations of $\{x_k\}$; (28) and (29)
$G(f), \bar{G}(f)$	Spectra of $\{x_k\}$; (31) and (32)
$\hat{\epsilon}_k, \tilde{\epsilon}_k$	Errors in prediction

FORTRAN PROGRAM FOR LINEAR PREDICTIVE SPECTRAL
ANALYSIS OF A COMPLEX UNIVARIATE PROCESS

1. INTRODUCTION

Spectral analysis of a complex univariate process via linear predictive and maximum entropy techniques is considered in reference 1, and Fortran programs for real data are presented there in appendix J. In this report, we present a program for handling the case of complex data, yielding as an output the auto-spectrum of the process.* Complex data can be encountered, for example, when a narrowband real process is complex-demodulated to a low frequency and sampled at a rate comparable to the bandwidth of the process. When the new center frequency is zero, the process is called the complex envelope.

In section 2, an example of the use of the program is presented, and the changes that the user must make for his application are pointed out. In section 3, the possibility of using this program to estimate the cross-spectrum of two real processes is investigated and found to be undesirable. In section 4, a limitation of the complex predictive filter for complex waveform estimation is considered, and a possible generalization is indicated to alleviate the problem.

*The theory and notation for this case were developed fully in reference 1 and will not be repeated here, for sake of brevity; the reader is referred to that earlier material for all details.

2. USE OF PROGRAM FOR SPECTRAL ANALYSIS

The program for spectral analysis of a complex process consists of five parts: a main program and four subroutines, as listed in appendix A. Input parameters to the main program (listed in statement 15) are

N, number of complex data points,
PMAX, maximum order of filter considered, and
J, size of FFT for spectral estimate.

The sample program generates a data example in lines 20-33 and must be replaced by the user to fit his particular applications.

A sample output for $N = 100$, $PMAX = 10$, is presented below. It indicates that $PBEST = 1$, which agrees with the actual value of p (see statement 21 of the main program). The fractional powers sum up to 0.99999829 instead of 1; the difference is a measure of whether the spectral estimate has been adequately sampled in frequency. (If the error is too large, J may be increased.)

Since the autospectrum of a complex process is real, but not necessarily even, it is necessary to compute the spectrum over both negative and positive frequencies. Thus bin 1 corresponds to zero frequency; bin $J/2 + 1$ corresponds to \pm Nyquist frequency, $\pm 1/(2\Delta)$; and bin J corresponds to frequency $-1/(J\Delta)$, where Δ is the sampling interval in time.

An example of a spectral estimate of 1000 samples of a complex envelope of surface-bottom forward scatter at a 20° grazing angle at frequency 750 Hz over a 20 nautical-mile path is presented in figure 1, where the sampling rate is 1 Hz. There is observed to be a pair of spectral peaks at $\pm 1/4$ Nyquist frequency, a strong very low frequency component, and a rather symmetric spectrum about zero frequency. In figure 2, the direct path is employed instead, the sampling rate is 0.1 Hz, but 1000 samples are still used. The center portion of the spectral estimate reveals a double peak near zero frequency and a rapid drop-off away from this frequency. With these few data points, resolution capability of this quality is very hard to achieve by any other spectral analysis techniques.

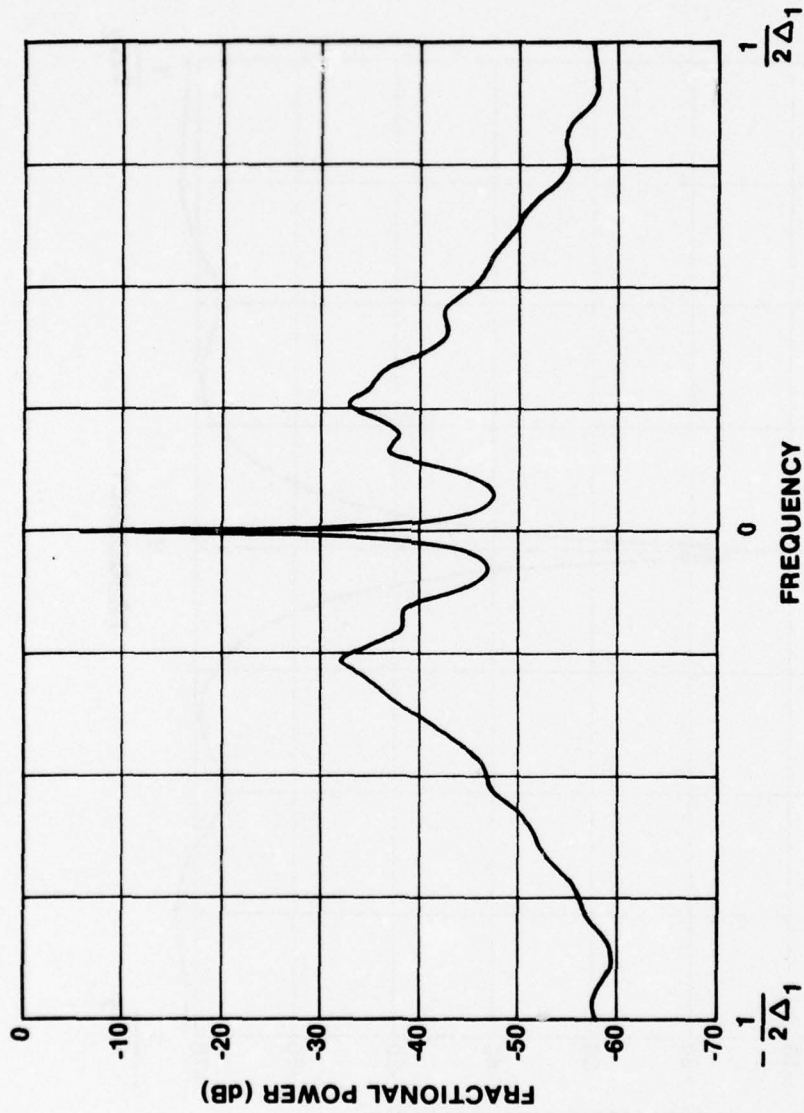


Figure 1. Spectrum of Surface-Bottom Forward Scatter

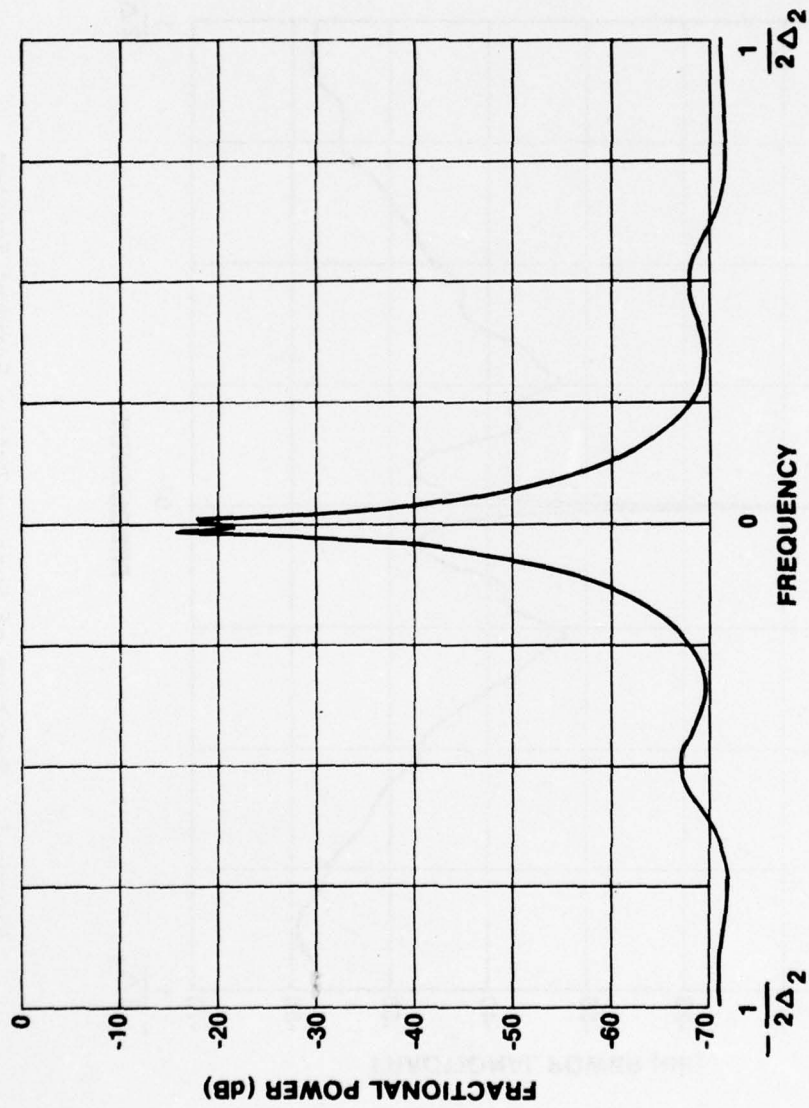


Figure 2. Spectrum of Direct Path

3. ESTIMATION OF CROSS-SPECTRUM OF TWO REAL PROCESSES

Suppose that processes $u(t)$ and $v(t)$ are real, zero-mean, and stationary. If we form the complex process

$$x(t) = \alpha u(t) + \beta v(t), \quad (1)$$

where α and β are complex, then the autocorrelation of $x(t)$ is

$$\begin{aligned} R_{xx}(\tau) &\equiv \overline{x(t)x^*(t-\tau)} = R_{xx}^*(-\tau) \\ &= |\alpha|^2 R_{uu}(\tau) + |\beta|^2 R_{vv}(\tau) + \alpha\beta^* R_{uv}(\tau) + \alpha^*\beta R_{uv}(-\tau), \end{aligned} \quad (2)$$

where the crosscorrelation of $u(t)$ and $v(t)$ is

$$R_{uv}(\tau) \equiv \overline{u(t)v(t-\tau)}. \quad (3)$$

The auto-spectrum of $x(t)$ is the nonnegative real (noneven) function

$$\begin{aligned} G_{xx}(f) &\equiv \int_{-\infty}^{\infty} d\tau \exp(-i2\pi f\tau) R_{xx}(\tau) \\ &= |\alpha|^2 G_{uu}(f) + |\beta|^2 G_{vv}(f) + \alpha\beta^* G_{uv}(f) + \alpha^*\beta G_{uv}^*(f), \end{aligned} \quad (4)$$

where the cross-spectrum of $u(t)$ and $v(t)$ is

$$G_{uv}(f) \equiv \int_{-\infty}^{\infty} d\tau \exp(-i2\pi f\tau) R_{uv}(\tau) = G_{uv}^*(-f). \quad (5)$$

Now let us decompose the cross-spectrum as

$$G_{uv}(f) = R(f) + iI(f), \quad (6)$$

for which (5) yields

$$R(-f) = R(f), \quad I(-f) = -I(f). \quad (7)$$

Utilizing (6) and (7) in (4), we obtain

$$\begin{aligned}
 G_{xx}(f) &= |\alpha|^2 G_{uu}(f) + |\beta|^2 G_{vv}(f) \\
 &\quad + 2\operatorname{Re}(\alpha\beta^*)R(f) - 2\operatorname{Im}(\alpha\beta^*)I(f), \\
 G_{xx}(-f) &= |\alpha|^2 G_{uu}(f) + |\beta|^2 G_{vv}(f) \\
 &\quad + 2\operatorname{Re}(\alpha\beta^*)R(f) + 2\operatorname{Im}(\alpha\beta^*)I(f).
 \end{aligned} \tag{8}$$

Solving (8) for $R(f)$ and $I(f)$, the real and imaginary parts, respectively, of cross-spectrum $G_{uv}(f)$, we obtain

$$\begin{aligned}
 R(f) &= \frac{1}{4} \frac{1}{\operatorname{Re}(\alpha\beta^*)} [G_{xx}(f) + G_{xx}(-f) - 2|\alpha|^2 G_{uu}(f) - 2|\beta|^2 G_{vv}(f)], \\
 I(f) &= -\frac{1}{4} \frac{1}{\operatorname{Im}(\alpha\beta^*)} [G_{xx}(f) - G_{xx}(-f)],
 \end{aligned} \tag{9}$$

if $\operatorname{Re}(\alpha\beta^*) \neq 0$ and $\operatorname{Im}(\alpha\beta^*) \neq 0$. Since α and β are arbitrary, we choose $\alpha\beta^* = (1 - i)/2$, for which $|\alpha|^2|\beta|^2 = |\alpha\beta^*|^2 = 1/2$. For simplicity, we choose $|\alpha|^2 = |\beta|^2 = 1/\sqrt{2}$; then (9) becomes

$$\begin{aligned}
 R(f) &= \frac{G_{xx}(f) + G_{xx}(-f)}{2} - \frac{G_{uu}(f) + G_{vv}(f)}{\sqrt{2}} \\
 &= \operatorname{EVEN}\{G_{xx}(f)\} - \frac{G_{uu}(f) + G_{vv}(f)}{\sqrt{2}}, \\
 I(f) &= \frac{G_{xx}(f) - G_{xx}(-f)}{2} = \operatorname{ODD}\{G_{xx}(f)\}.
 \end{aligned} \tag{10}$$

Now we need only compute $R(f)$ and $I(f)$ for $f \geq 0$, as (7) indicates.

An alternative method to (10) was presented in reference 2, equation (4). However, that method required calculating four auto-spectra, whereas the current method requires calculating only three auto-spectra: $G_{uu}(f)$ and $G_{vv}(f)$ are real and even, whereas $G_{xx}(f)$ is real, but not necessarily even.

The choices of α and β in (1) are still not unique. If we let

$$\alpha = 2^{-1/4} e^{i\theta}, \quad \beta = 2^{-1/4} e^{i\phi}, \quad (11)$$

then

$$\alpha\beta^* = 2^{-1/2} e^{i(\theta-\phi)} = \frac{1-i}{2} = 2^{-1/2} e^{-i\pi/4}. \quad (12)$$

Therefore, we must have $\theta - \phi = -\pi/4$. There are two obvious choices:

Choice 1

$$\theta = 0, \quad \phi = \pi/4$$

$$\alpha = 2^{-1/4}, \quad \beta = 2^{-1/4} \left(\frac{1+i}{\sqrt{2}} \right)$$

$$x(t) = 2^{-1/4} \left[u(t) + \frac{1+i}{\sqrt{2}} v(t) \right], \quad (13)$$

which is not very symmetric.

Choice 2

$$\theta = -\pi/8, \quad \phi = \pi/8$$

$$\alpha = 2^{-1/4} e^{-i\pi/8} \equiv a - ib$$

$$\beta = 2^{-1/4} e^{i\pi/8} = a + ib$$

$$a = 2^{-1/4} \cos(\pi/8), \quad b = 2^{-1/4} \sin(\pi/8)$$

$$x(t) = a[v(t) + u(t)] + ib[v(t) - u(t)], \quad (14)$$

which is the preferred form.

For known autocorrelations or auto-spectra, (10) furnishes a valid way of calculating the real and imaginary parts of the cross-spectrum of real processes $u(t)$ and $v(t)$. However, when the auto-spectra are

unknown, spectral estimates must be substituted in (10). Although $R(f)$ and $I(f)$ can both take on positive or negative values in any frequency range, there is a constraint on their magnitudes. Namely, the magnitude-coherence is upper-bounded by unity. However, several numerical examples using the programs in appendix A, for cases where the true magnitude-coherence was near unity, yielded estimated magnitude-coherences greater than unity in some frequency ranges. This was traced to the fact that the estimate of $G_{xx}(f)$ can be too small and/or the estimates of $G_{uu}(f)$ and $G_{vv}(f)$ can be too large. This type of coherence estimate is intolerable; hence, estimation of cross-spectra of real processes by means of the auto-spectrum of a complex process is discouraged. The same conclusion is offered for the method in reference 2.

4. A LIMITATION OF COMPLEX PREDICTIVE FILTER

The theory behind the program presented in appendix A has been given in reference 1 and is based on a linear predictive technique. Specifically, given p past values of complex process $\{x_k\}$, a linear one-step prediction of x_k is attempted according to reference 1, equation 58:

$$\hat{x}_k \equiv \sum_{n=1}^p a_n x_{k-n}. \quad (15)$$

If we express all the quantities in (15) in terms of their real and imaginary parts according to definitions

$$\hat{x}_k = \hat{u}_k + i\hat{v}_k, \quad x_k = u_k + iv_k, \quad a_n = \alpha_n + i\beta_n, \quad (16)$$

then (15) can be expressed as

$$\begin{aligned} \hat{u}_k &= \sum_{n=1}^p (\alpha_n u_{k-n} - \beta_n v_{k-n}), \\ \hat{v}_k &= \sum_{n=1}^p (\beta_n u_{k-n} + \alpha_n v_{k-n}). \end{aligned} \quad (17)$$

But (17) is not as general as the form for prediction given by $(\mu_n, \nu_n, \beta_n, \alpha_n \text{ real})$:

$$\begin{aligned} \tilde{u}_k &= \sum_{n=1}^p (\mu_n u_{k-n} + \nu_n v_{k-n}), \\ \tilde{v}_k &= \sum_{n=1}^p (\beta_n u_{k-n} + \alpha_n v_{k-n}). \end{aligned} \quad (18)$$

It is apparent that the mean-square errors of predictions in (18) could be made smaller than those in (17), in general.

The complex estimate of x_k that can be formed from (18) is

$$\tilde{x}_k \equiv \tilde{u}_k + i\tilde{v}_k = \sum_{n=1}^p (g_n x_{k-n} + h_n x_{k-n}^*), \quad (19)$$

where

$$\begin{aligned} g_n &= \frac{1}{2}[\mu_n + \alpha_n + i(\beta_n - \nu_n)], \\ h_n &= \frac{1}{2}[\mu_n - \alpha_n + i(\beta_n + \nu_n)]. \end{aligned} \quad (20)$$

(The form (19) is the one alluded to in reference 1, footnote to equation (58).) The coefficients $\{g_n\}_1^p$ and $\{h_n\}_1^p$ in (19) are two completely independent sets of complex constants that can be chosen. Since the complex predictive filter in (15) is obviously a special case of (19), it is expected to have a more limited ability in waveform prediction than (19); however, (15) may suffice for spectral approximation purposes. (For a real process, (19) reduces to (15).)

Now suppose that a pair of real processes were actually generated according to p-th order autoregressions,

$$\begin{aligned} u_k &= \sum_{n=1}^p (\mu_n u_{k-n} + \nu_n v_{k-n}) + d_k, \\ \bar{v}_k &= \sum_{n=1}^p (\beta_n u_{k-n} + \alpha_n v_{k-n}) + b_k, \end{aligned} \quad (21)$$

where all the quantities are real. Then complex process

$$x_k \equiv u_k + iv_k = \sum_{n=1}^p (g_n x_{k-n} + h_n x_{k-n}^*) + w_k, \quad (22)$$

where g_n and h_n are given by (20), and

$$w_k \equiv d_k + ib_k. \quad (23)$$

Now if $\alpha_n = -\mu_n$, $\beta_n = \nu_n$, for $1 \leq n \leq p$ in (21), we get $g_n = 0$, $h_n = \mu_n + i\nu_n$, and (22) yields autoregression

$$x_k = \sum_{n=1}^p h_n x_{k-n}^* + w_k. \quad (24)$$

So a linear prediction according to (15) is not expected to do too well on the actual waveform values given by (24), no matter what the statistics of $\{w_k\}$ are. However, the spectral approximation available via (15) of $G_x(f)$ for process (24) can be very good if p is chosen large enough in (15).

As an example, let $p = 1$ in (24):

$$x_k = hx_{k-1}^* + w_k, \quad (25)$$

where h and w_k are complex with

$$|h| < 1, \quad (26a)$$

$$\overline{w_k w_{k-n}^*} = \delta_{0n}, \quad \overline{w_k w_{k-n}} = 0. \quad (26b)$$

The excitation process described in (26b) is an analytic process, as witnessed by the zero value for the second ensemble average. We find averages

$$\overline{w_k x_{k-n}} = 0, \quad \overline{w_k x_{k-n}^*} = \delta_{0n}, \quad n \geq 0, \quad (27)$$

and correlations

$$R_n \equiv \overline{x_k x_{k-n}^*} = \frac{1}{1 - |h|^2} \begin{cases} |h|^n, & n = 0, 2, 4, \dots \\ 0, & n = 1, 3, 5, \dots \end{cases}, \quad (28)$$

$$\mathcal{R}_n \equiv \overline{x_k x_{k-n}} = \frac{h}{1 - |h|^2} \begin{cases} 0, & n = 0, 2, 4, \dots \\ |h|^{n-1}, & n = 1, 3, 5, \dots \end{cases}. \quad (29)$$

Since (29) is not zero for all n , process $\{x_k\}$ of (25) is not an analytic process.

If we use the facts (derivable from the definitions above) that

$$R_{-n} = R_n^*, \quad \mathcal{R}_{-n} = \mathcal{R}_n, \quad (30)$$

we find that the spectra

$$\begin{aligned}
 G(f) &\equiv \Delta \sum_{n=-\infty}^{\infty} R_n \exp(-i2\pi fn\Delta) \\
 &= \Delta \frac{1 + |h|^2}{|1 - |h|^2 \exp(-i2\pi f2\Delta)|^2}, \quad (31)
 \end{aligned}$$

and

$$\begin{aligned}
 \mathbf{G}(f) &\equiv \Delta \sum_{n=-\infty}^{\infty} \mathbf{R}_n \exp(-i2\pi fn\Delta) \\
 &= \Delta \frac{2h \cos(2\pi f\Delta)}{|1 - |h|^2 \exp(-i2\pi f2\Delta)|^2}. \quad (32)
 \end{aligned}$$

Generally, spectrum $G(f)$ is real and positive and $\mathbf{G}(f)$ is complex and even about $f = 0$. For this particular example, (25), $G(f)$ is also even about $f = 0$.

If we attempt prediction on the process (25) according to (15) and we minimize

$$\overline{|\hat{\epsilon}_k|^2} \equiv \overline{|\hat{x}_k - x_k|^2}, \quad (33)$$

we find

$$\hat{a}_n = \begin{cases} 0, & n \neq 2 \\ |h|^2, & n = 2 \end{cases} \quad (34)$$

and

$$\min \overline{|\hat{\epsilon}_k|^2} = \begin{cases} (1 - |h|^2)^{-1}, & p = 1 \\ 1 + |h|^2, & p \geq 2 \end{cases}. \quad (35)$$

Now (34) is hardly the same result as the actual autoregression (25). Nevertheless we find spectral approximation

$$\hat{G}(f) = \begin{cases} \Delta(1 - |h|^2)^{-1}, & p = 1 \\ G(f), & p \geq 2 \end{cases}, \quad (36)$$

from (34); that is, the spectral approximation is exact for $p \geq 2$, despite the obvious error of (34) in terms of waveform prediction.

If instead we attempt prediction on process (25) according to (19) and we minimize

$$\overline{|\tilde{\epsilon}_k|^2} \equiv \overline{|\tilde{x}_k - x_k|^2}, \quad (37)$$

we find, of course,

$$g_n = 0, \quad h_n = \begin{cases} 0, & n \neq 1 \\ h, & n = 1 \end{cases} \quad (38)$$

and

$$\min \overline{|\tilde{\epsilon}_k|^2} = 1 = \overline{|w_k|^2}. \quad (39)$$

For $|h|^2$ near 1, the error (35) for $p \geq 2$ is approximately twice as great as (39).

For the general autoregression in (22), it is shown in appendix B that for analytic white noise $\{w_k\}$, $\{h_n\}_1^p = 0$ if and only if $\{\hat{R}_m\}_0^p = 0$. Thus, given a complex data sequence $\{x_n\}_1^N$ of unknown origin, we can define

$$\hat{R}_m \equiv \frac{1}{N-m} \sum_{n=m+1}^N x_n x_{n-m}^*, \quad 0 \leq m,$$

$$\hat{R}_0 \equiv \frac{1}{N} \sum_{n=1}^N |x_n|^2. \quad (40)$$

Then, if $|\hat{R}_m|/\hat{R}_0 \ll 1$ for $0 \leq m \leq q$, the autoregressive model (19) with $\{h_n\}_1^p = 0$ can be used with some confidence for $p \leq q$ to predict the actual waveform. But, even if some $\hat{R}_m \neq 0$, the autoregressive model (19) with $\{h_n\}_1^p = 0$ can still be used to estimate the spectrum of the process

$\{x_k\}$; however, in order to attain equivalent spectral estimates, it has been observed that more data points, N , are needed when some $h_n \neq 0$ than when $\{h_n\}_1^p = 0$.

If a process is generated according to autoregression

$$x_k = \sum_{n=1}^p g_n x_{k-n} + w_k, \quad (41)$$

where process $\{w_k\}$ is not analytic, then $\{R_m\}$ are not necessarily zero. Thereby prediction (15) will not necessarily give accurate predictions, although the spectral estimate can still be adequate; this situation is discussed further in appendix C. Generation of analytic processes is considered in appendix D, and a more thorough look at the prediction capability of (19) is considered in appendix E.

5. DISCUSSION

A program for estimating the autospectrum of a complex univariate process via linear predictive techniques has been presented. Although it can be used to estimate the cross-spectrum of two real processes, it is not recommended because estimated values of magnitude-coherence greater than unity can result. Instead, the methods of multivariate techniques presented in reference 3 should be employed; in fact, the theory for complex multivariate processes is developed there and a working program given.

Although the program presented here presumes that none of the data points are bad, it may be readily generalized to include bad data points. The method and program presented in reference 1 furnish the necessary background for this extension.

Application of the linear predictive technique in (15) is most successful when the complex process under investigation is analytic. Otherwise, the more general prediction technique in (19) is worthy of consideration.

Appendix A

FORTRAN PROGRAM FOR SPECTRAL ANALYSIS

The following program for spectral analysis of a complex process consists of five parts: a main program and four external subroutines. The subroutine BURGEX computes the complex predictive filter coefficients, POWERC computes the fractional power in bands $(J\Delta)^{-1}$ Hz wide, MKLFFT effects a fast Fourier transform (reference 4), and QTRCOS generates a table of cosine values (reference 4).

```

C SPECIAL ESTIMATION FOR COMPLEX DATA
C USE: CHANGE LINE 15 AND REPLACE LINES 20-33
C N = NUMBER OF COMPLEX DATA POINTS; INTEGER INPUT
C X(1),...,X(N) = COMPLEX INPUT DATA; ALTERED OR OUTPUT
C PMAX = MAXIMUM ORDER OF FILTER; INTEGER INPUT
C J = SIZE OF FFT (MUST BE A POWER OF 2 TO USE R(LEFT)); INTEGER INPUT
C PBEST = BEST ORDER OF FILTER; INTEGER OUTPUT
C A(1),...,A(PBEST) = COMPLEX PREDICTIVE FILTER COEFFICIENTS; OUTPUT
C PROD = PRODUCT(1-ABS(A(P))**2) FOR P=1 TO PBEST; OUTPUT
C RHO(1),...,RHO(PMAX) = COMPLEX NORMALIZED CORRELATIONS; OUTPUT
C XX(1),...,XX(J) = FRACTIONAL POWERS; OUTPUT
C CO(1),...,CO(J/4+1) = QUARTER COSINE TABLE FOR FFT PURPOSES
C Y IS A REQUIRED COMPLEX AUXILIARY ARRAY
C YY IS A REQUIRED AUXILIARY ARRAY
      PARAMETER N=100, PMAX=10, J=512, J41=J/4+1
      INTEGER PBEST
      COMPLEX X(N), Y(N), A(PMAX), RHO(PMAX)
      DIMENSION XX(J), YY(J), CO(J41)
C COMPLEX INPUT DATA IN X(1),...,X(N)
      COMPLEX A1,Z(1400)
      DEFINE IRAND=I*5**15+((1-SIGN(1,I*5**15))/2)*34359738367
      DEFINE RAND=FLOAT(1)/34359738367.
      I=5281
      A1=(.65,.65)
      Z(1)=(0.,0.)
      DO 21 L=2,1400
        I=IRAND
        R1=RAND-.5
        I=IRAND
        R2=RAND-.5
21      Z(L)=A1*Z(L-1)+CMPLX(R1,R2)
      DO 22 I=1,N
22      X(I)=Z(I+1400-N)
      PRINT 1
1      FORMAT(1H1,' INPUT DATA:')
      PRINT 4, (X(I),I=1,N)
C EVALUATE PREDICTIVE FILTER COEFFICIENTS
      CALL BURGCX(N,PMAX,X,Y,PBEST,A,PROD,RHO)
      PRINT 9, X(N)
9      FORMAT(/' MEAN = (' ,E13.8,' ,',E13.8,')')
      R1=REAL(Y(N))
      PRINT 10, R1
10     FORMAT(' STANDARD DEVIATION =',E13.8)
      PRINT 2, PBEST
2      FORMAT(/' PBEST =',I3)
      IF(PBEST,EQ.0) GO TO 12
      PRINT 3
3      FORMAT(/' PREDICTIVE FILTER COEFFICIENTS FOR PBEST:')
      PRINT 4, (A(I),I=1,PBEST)
4      FORMAT(4(E18.8,E15.8))
12     PRINT 5, PROD

```

```

5   FORMAT(/' PRODUCT(1-ABS(A(P))**2) =' ,E13.6)
   PRINT 6
6   FORMAT(/' NORMALIZED CORRELATION COEFFICIENTS:')
   PRINT 4, (RHO(I),I=1,PMAX)
   CALL QTRCOS(CO,J)
C   EVALUATE FRACTIONAL POWERS
   CALL POWERC(PBEST,A,PROD,J,XX,YY,CO,SUM)
   PRINT 7
7   FORMAT(/' FRACTIONAL POWERS:')
   PRINT 8, (XX(I),I=1,J)
8   FORMAT(2X,10E13.6)
   PRINT 11, SUM
11  FORMAT(/' SUM OF FRACTIONAL POWERS =' ,E13.6)
   END

```

```

SUBROUTINE FURCOX(N,PMAX,X,Y,PBEST,A,PROD,RHO)
C THIS SUBROUTINE COMPUTES THE COMPLEX PREDICTIVE FILTER COEFFICIENTS
C N = NUMBER OF COMPLEX DATA POINTS; INTEGER INPUT
C PMAX = MAXIMUM ORDER OF FILTER; INTEGER INPUT
C X(1),X(2),...,X(N) = COMPLEX DATA ARRAY ON INPUT; ALTERED ON OUTPUT
C ON OUTPUT, X(1),X(2),...,X(PMAX) = A(1;PMAX),A(2;PMAX),...,A(PMAX;PMAX)
C Y(1),Y(2),...,Y(N) = COMPLEX AUXILIARY ARRAY; SCRATCH INPUT
C ON OUTPUT, Y(1),Y(2),...,Y(PMAX) = A(1;1),A(2;2),...,A(PMAX;PMAX)
C ON OUTPUT, X(N) = MEAN, AND Y(N) = STANDARD DEVIATION OF INPUT DATA
C PBEST = BEST ORDER OF FILTER; INTEGER OUTPUT
C A(1),A(2),...,A(PBEST) = COMPLEX PREDICTIVE FILTER COEFFICIENT ARRAY =
C A(1;PBEST),A(2;PBEST),...,A(PBEST;PBEST); OUTPUT
C PROD = PRODUCT(1-ABS(A(P;PBEST))**2) FOR P=1 TO PBEST; OUTPUT
C RHO(1),...,RHO(PMAX) = COMPLEX NORMALIZED CORRELATIONS; OUTPUT
C COMPLEX X(N),Y(N),A(PMAX),RHO(PMAX) IS REQUIRED IN MAIN PROGRAM
   INTEGER PMAX,PBEST,P
   DOUBLE PRECISION SA,SA1,SB
   COMPLEX S1,G,T
   COMPLEX X(1),Y(1),A(1),RHO(1)
   IF(PMAX.GT.3.*SQRT(N)) PRINT 2, PMAX,N
2   FORMAT(/' PMAX =' ,14,' IS TOO LARGE FOR NUMBER OF DATA POINTS II ='
   $,15)
C COMPUTE MEAN
   S1=(0.,0.)
   DO 1 I=1,N
1   S1=S1+X(I)
   S1=CMPLX(REAL(S1)/N,AIMAG(S1)/N)
C SUBTRACT MEAN, AND SCALE TO UNIT VARIANCE
   S2=0.
   DO 3 I=1,N
3   S2=S2+REAL(X(I)-S1)**2+AIMAG(X(I)-S1)**2
   S2=SQRT(S2/(N-1.))
   B=1./S2
   DO 5 I=1,N
5   A(I)=CMPLX(REAL(X(I))*B,AIMAG(X(I))*B)
   Y(1)=X(1)

```

TR 5505

```
C BEGIN RECURSION
  F=0
  PRODU=1.
  AICMIN=0.
  PBEST=0
  PRD=1.
  P=P+1
C CALCULATE CROSS-GAIN; EQ. 155
  SAR=0.D0
  SAI=0.D0
  SB=0.D0
  L=P+1
  DO 7 I=L,N
    T1=REAL(X(I))
    T2=AIMAG(X(I))
    T3=REAL(Y(I-1))
    T4=AIMAG(Y(I-1))
    SAR=SAR+T1*T3+T2*T4
    SAI=SAI+T2*T3-T1*T4
  7 SB=SB+T1**2+T2**2+T3**2+T4**2
    F=2.*SAR/SB
    C=2.*SAI/SB
    G=CMPLX(B,C)
    B=1.-B*B*C*C
    PRODU=PRODU*B
C CALCULATE FILTER COEFFICIENTS; EQS. 160&148. STORE IN X(1),...,X(P)
  X(P)=G
  IF(P.EQ.1) GO TO 8
  L=P/2
  DO 9 I=1,L
    T=X(I)-G*CONJG(X(P-I))
    X(P-I)=X(P-I)-G*CONJG(X(I))
  9 X(I)=T
C CALCULATE NORMALIZED CORRELATION COEFFICIENT; EQ. 149
  T=X(P)
  IF(P.EQ.1) GO TO 14
  L=P-1
  DO 15 I=1,L
    T=T+X(I)*RHO(P-I)
  15 RHO(P)=T
  14 RHO(P)=T
C CALCULATE AKAIKE'S INFORMATION CRITERION; EQS. 156&202
  RELEBR=B*SNGL(SB)/(2.*(N-P))
  AIC=LOG(RELEBR)+4.*FLOAT(P)/(N-P)
  IF(AIC.GE.AICMIN) GO TO 10
  AICMIN=AIC
  PBEST=P
  PRD=PRODU
  DO 11 I=1,P
    11 A(I)=X(I)
  10 IF(P.EQ.PMAX) GO TO 16
C UPDATE FORWARD AND BACKWARD SEQUENCES; EQ. 153
  L=P+1
  DO 12 I=N,L,-1
    T=X(I)-G*Y(I-1)
    Y(I)=Y(I-1)-CONJG(G)*X(I)
```

```

12   X(I)=T
      Y(P)=G
      GO TO 6
16   Y(PMAX)=G
      IF(PBEST,EG,PMAX) GO TO 4
C   COMPUTE EXTRAPOLATED NORMALIZED CORRELATION
C   COEFFICIENTS FROM PBEST+1 TO PMAX; EQ. 165
      L=PBEST+1
      DO 17 P=L,PMAX
        A(P)=(0.,0.)
        T=(0.,0.)
      DO 18 I=1,PBEST
18   T=T+A(I)*RHO(P-I)
17   RHO(P)=T
      X(N)=S1
      Y(N)=CMPLX(S2,0.)
      RETURN
      END

```

```

      SUBROUTINE POWERC(PBEST,A,PROD,J,XX,YY,CC,SU)
C   THIS SUBROUTINE COMPUTES THE FRACTIONAL POWERS IN BANDS 1/(J*DELTA)
C   PBEST = BEST ORDER OF FILTER; INTEGER INPUT
C   A(1),...,A(PBEST) = COMPLEX FILTER COEFFICIENT ARRAY; INPUT
C   PROD = PRODUCT(1-ABS(A(P))**2) FOR P=1 TO PBEST; INPUT
C   J = SIZE OF FFT; INTEGER INPUT
C   XX = AUXILIARY ARRAY ON INPUT
C   XX(1),...,XX(J) = FRACTIONAL POWERS OF; OUTPUT
C   YY = AUXILIARY ARRAY; SCRATCH INPUT
C   CC(1),...,CC(J/4+1) = QUARTER COSINE TABLE FOR FFT; INPUT
C   DIMENSION YX(J),YY(J),CC(J/4+1) IS REQUIRED IN MAIN PROGRAM
C   COMPLEX A(PMAX) IS REQUIRED IN MAIN PROGRAM, WHERE PMAX.GE.PBEST
      INTEGER PBEST
      DIMENSION XX(1),YY(1),CC(1)
      COMPLEX A(1)
      F=PROD/J
      XX(1)=1.
      YY(1)=0.
      IF(PBEST,EG,0) GO TO 4
      DO 1 I=1,PBEST
1   XX(I+1)=REAL(A(I))
      YY(I+1)=-A1*AG(A(I))
4   L=PBEST+2
      DO 2 I=L,J
2   XX(I)=0.
      YY(I)=0.
      L=1.4427*LOG(J)+.5 @ LOG2(J)
      CALL FRLFFT(XX,YY,CC,L,-1)
      SUM=0.
      DO 3 I=1,J
3   XX(I)=F/(XX(I)**2+YY(I)**2)
      SUM=SUM+XX(I)
      RETURN
      END

```

TR 5505

```
SUBROUTINE MKLEFT(X,Y,CC,M,ISN)
DIMENSION X(1),Y(1),CC(1),L(12)
EQUIVALENCE (L12,L(1)),(L11,L(2)),(L10,L(3)),(L9,L(4)),(L8,L(5)),
1(L7,L(6)),(L6,L(7)),(L5,L(8)),(L4,L(9)),(L3,L(10)),(L2,L(11)),
2(L1,L(12))
I=2**M
ND4=N/4
ND4P1=ND4+1
ND4P2=ND4P1+1
ND2P2=ND4+ND4P2
DO 8 LO=1,M
LMA=2**(M-LO)
LIX=2*L/X
ISCL=N/LIX
DO 8 LM=1,LMX
IARG=(LM+1)*ISCL+1
IF(IARG,LE,ND4P1) GO TO 4
C=-CC(ND2P2-IARG)
S=ISN*CC(IARG-ND4)
GO TO 6
4 C=CC(IARG)
S=ISN*CC(ND4P2-IARG)
6 DO 8 LI=LIX,N,LIX
J1=LI-LIX+LM
J2=J1+L/X
T1=X(J1)*X(J2)
T2=Y(J1)*Y(J2)
X(J1)=X(J1)+X(J2)
Y(J1)=Y(J1)+Y(J2)
X(J2)=C*T1-S*T2
Y(J2)=C*T2+S*T1
8 CONTINUE
DO 40 J=1,12
L(J)=1
IF(J=?) 31,31,40
31 L(J)=2**(M+1-J)
40 CONTINUE
JN=1
DO 60 J1=1,L1
DO 60 J2=J1,L2,L1
DO 60 J3=J2,L3,L2
DO 60 J4=J3,L4,L3
DO 60 J5=J4,L5,L4
DO 60 J6=J5,L6,L5
DO 60 J7=J6,L7,L6
DO 60 J8=J7,L8,L7
DO 60 J9=J8,L9,L8
DO 60 J10=J9,L10,L9
DO 60 J11=J10,L11,L10
DO 60 J12=J11,L12,L11
IF(JN=J1) 51,51,52
51 F=X(JN)
X(JN)=X(J1)
X(J1)=F
F=Y(JN)
```

```
Y(JR)=Y(JR)
Y(JR)=F I
52 JN=JN+1
60 CONTINUE
RETURN
END
```

```
SUBROUTINE QTRCOS(C,N)
DIMENSION C(1)
I+1=N/4+1
SCL=6.283185307/N
DO 1 I=1,N/4
C(I)=COS((I-1)*SCL)
RETURN
END
```

Appendix B

PROPERTY OF AUTOREGRESSIVE MODEL

The process of interest here is given by the autoregressive model (22):

$$x_k = \sum_{n=1}^p (g_n x_{k-n} + h_n x_{k-n}^*) + w_k, \quad (\text{B-1})$$

where excitation $\{w_k\}$ is analytic white noise. That is,

$$\overline{w_k w_{k-m}^*} = \delta_{om}, \quad \overline{w_k w_{k-m}} = 0. \quad (\text{B-2})$$

It then follows easily that

$$\overline{w_k x_{k-m}^*} = \delta_{om}, \quad \overline{w_k x_{k-m}} = 0, \quad m \geq 0. \quad (\text{B-3})$$

Use of (B-2) and (B-3) then yields correlations

$$R_m \equiv \overline{x_k x_{k-m}} = \sum_{n=1}^p (g_n R_{m-n} + h_n R_{m-n}^*), \quad m \geq 0, \quad (\text{B-4})$$

$$R_m \equiv \overline{x_k x_{k-m}^*} = \sum_{n=1}^p (g_n R_{m-n} + h_n R_{m-n}^*) + \delta_{om}, \quad m \geq 0. \quad (\text{B-5})$$

For given coefficients $\{g_n\}_1^p$ and $\{h_n\}_1^p$, (B-4) and (B-5) constitute simultaneous equations in the unknown correlations.

Now let us suppose that

$$h_n = 0, \quad 1 \leq n \leq p. \quad (\text{B-6})$$

Then, from (B-4), the first $p + 1$ equations yield

$$\begin{aligned}
 R_0 - g_1 R_1 - \dots - g_p R_p &= 0 \\
 \vdots & \\
 R_p - g_1 R_{p-1} - \dots - g_p R_0 &= 0.
 \end{aligned}
 \tag{B-7}$$

Therefore

$$R_m = 0, \quad 0 \leq m \leq p, \tag{B-8}$$

and from (B-4) and (B-6) it follows that R_m is zero for all m .

Conversely, assume that

$$R_m = 0, \quad 0 \leq m \leq p. \tag{B-9}$$

Then, from (B-4), the first p equations yield

$$\begin{aligned}
 h_1 R_1 + h_2 R_2 + \dots + h_p R_p &= 0 \\
 \vdots & \\
 h_1 R_{2-p} + h_2 R_{3-p} + \dots + h_p R_1 &= 0.
 \end{aligned}
 \tag{B-10}$$

Therefore

$$h_n = 0, \quad 1 \leq n \leq p, \tag{B-11}$$

and from (B-4) and (B-11) it follows that R_m is zero for all m .

Thus we have shown that $\{h_n\}_1^p = 0$ if and only if $\{R_m\}_0^p = 0$ in the autoregression (B-1) with analytic white noise excitation.

Appendix C

NONANALYTIC WHITE NOISE EXCITATION

Suppose a process is generated according to autoregression

$$x_k = \sum_{n=1}^p g_n x_{k-n} + w_k, \quad (C-1)$$

where excitation $\{w_k\}$ satisfies

$$\overline{w_k w_{k-m}^*} = B \delta_{0m} \quad \overline{w_k w_{k-m}} = \mathcal{B} \delta_{0m}. \quad (C-2)$$

\mathcal{B} is complex and nonzero; therefore $\{w_k\}$ is not an analytic process, although it is white.

Then $\{R_m\}$ need not equal zero, even for autoregression (C-1). For example, for

$$p = 1, g_1 = g, |g| < 1, g \text{ complex}, \quad (C-3)$$

we find correlations

$$R_0 = \frac{B}{1 - |g|^2}, \quad R_m = g^m R_0, \quad m \geq 1, \quad R_{-m} = R_m^*, \quad (C-4)$$

$$R_0 = \frac{\mathcal{B}}{1 - g^2}, \quad R_m = g^m R_0, \quad m \geq 1, \quad R_{-m} = R_m. \quad (C-5)$$

The corresponding spectra are

$$G(f) = \frac{\Delta B}{|1 - g e^{-i2\pi f \Delta}|^2}, \quad (C-6)$$

$$G(f) = \frac{\Delta \mathcal{B}}{1 - 2g \cos(2\pi f \Delta) + g^2}. \quad (C-7)$$

Since the $\{R_m\}$ are not zero, appendix B shows that the coefficients $\{h_n\}$ would not be zero in model (B-1) with an analytic excitation.

Optimum prediction on process (C-1) using (15) gives

$$\hat{a}_n = \begin{cases} g, & n = 1 \\ 0, & n \neq 1 \end{cases}, \quad (\text{C-8})$$

with a minimum mean square error equal to B, and the spectral estimate is identically (C-6). Thus, for this example, the nonanalyticity of the excitation is no problem.

For the more general model of (C-1) with $p > 1$, it can be shown that all $\{R_m\}$ are independent of the value of \mathcal{B} . Then, although (15) may not be too accurate for waveform prediction, it can still be used for spectral estimation purposes.

Optimum prediction on process (C-1) using (19) gives

$$\hat{g}_1 = g, \quad \text{other coefficients} = 0, \quad (\text{C-9})$$

with a minimum mean square error equal to B. This yields the same result as above.

Appendix D

A METHOD OF GENERATING ANALYTIC PROCESSES

Suppose linear filter $H(f)$ is excited by complex input $x(t)$, yielding output $y(t)$. Then correlation

$$R_y(\tau) \equiv \overline{y(t)y^*(t-\tau)} = \int df \exp(i2\pi f\tau) G_x(f) |H(f)|^2, \quad (D-1)$$

and spectrum

$$G_y(f) \equiv \int d\tau \exp(-i2\pi f\tau) R_y(\tau) = G_x(f) |H(f)|^2. \quad (D-2)$$

Also correlation

$$\begin{aligned} R_y(\tau) &\equiv \overline{y(t)y(t-\tau)} \\ &= \int df \exp(i2\pi f\tau) G_x(f) H(f) H(-f), \end{aligned} \quad (D-3)$$

and spectrum

$$G_y(f) \equiv \int d\tau \exp(-i2\pi f\tau) R_y(\tau) = G_x(f) H(f) H(-f). \quad (D-4)$$

Complex process $y(t)$ is defined as being analytic if (D-3) is zero for all τ . Suppose that filter

$$H(f) = 0 \text{ for } f < 0. \quad (D-5)$$

Denote the output of filter (D-5) by $y_+(t)$. Then (D-4) shows that $G_y(f)$ and $R_y(\tau)$ are both identically zero for all argument values. Therefore single-sided waveform $y_+(t)$ is an analytic process.

Let complex envelope

$$\underline{y}(t) \equiv y_+(t) \exp(-i2\pi f_0 t). \quad (D-6)$$

Then

$$R_y(\tau) \equiv \overline{y(t)y^*(t-\tau)} = R_{y+}(\tau) \exp(-i2\pi f_0 \tau) = 0 \quad (D-7)$$

for any f_0 . Thus the complex envelope of any stationary process is an analytic process.

On the other hand, for the two real processes $u(t)$ and $v(t)$, no linear combination, $\alpha u(t) + \beta v(t)$, where α and β are complex, ever yields an analytic process unless $R_{uu}(\tau)$, $R_{vv}(\tau)$, and $R_{uv}(\tau)$ satisfy very special restrictions. Thus the process constructed in (1) was not analytic and could not have been expected to yield good prediction capability via (15).

Appendix E

CAPABILITY OF A MORE GENERAL PREDICTION MODEL

If p is infinite in (19), we have prediction

$$\tilde{x}_k = \sum_{n=1}^{\infty} (g_n x_{k-n} + h_n x_{k-n}^*). \quad (\text{E-1})$$

Minimization of $\overline{|\tilde{\epsilon}_k|^2} \equiv \overline{|\tilde{x}_k - x_k|^2}$ yields the simultaneous equations

$$\sum_{n=1}^{\infty} (g_n R_{m-n} + h_n R_{m-n}^*) = R_m, \quad 1 \leq m,$$

$$\sum_{n=1}^{\infty} (g_n R_{m-n} + h_n R_{m-n}^*) = R_m, \quad 1 \leq m. \quad (\text{E-2})$$

It can then be shown that $\tilde{\epsilon}_k$ is a white process with

$$\min \overline{|\tilde{\epsilon}_k|^2} = R_0 - \sum_{n=1}^{\infty} (g_n R_n^* + h_n R_n^*). \quad (\text{E-3})$$

Also it can be shown that

$$\overline{\tilde{\epsilon}_k \tilde{\epsilon}_{k-m}} = 0 \quad \text{for } m \neq 0, \quad (\text{E-4})$$

with

$$\overline{\tilde{\epsilon}_k^2} = R_0 - \sum_{n=1}^{\infty} (g_n R_n + h_n R_n). \quad (\text{E-5})$$

However, $\tilde{\epsilon}_k$ is not an analytic process since (E-5) is not zero. The simplest example to demonstrate this is

$$R_n = R_0 \delta_{0n}, \quad R_n^* = R_0 \delta_{0n}, \quad (\text{E-6})$$

for which (E-3) and (E-5) yield R_0 and R_0 , respectively.

The spectral relations for (E-1) take the forms

$$G_{\bar{x}}(f) = G_x(f) |A(f)|^2 + G_x(-f) |B(f)|^2 + \mathbf{G}_x(f) A(f) B^*(f) + [\mathbf{G}_x(f) A(f) B^*(f)]^* \quad (E-7)$$

and

$$\mathbf{G}_{\bar{x}}(f) = \mathbf{G}_x(f) A(f) A(-f) + \mathbf{G}_x^*(f) B(f) B(-f) + G_x(f) A(f) B(-f) + G_x(-f) A(-f) B(f), \quad (E-8)$$

where

$$A(f) \equiv \sum_{n=1}^{\infty} g_n \exp(-i2\pi f n \Delta)$$

and

$$B(f) \equiv \sum_{n=1}^{\infty} h_n \exp(-i2\pi f n \Delta) \quad (E-9)$$

are considered known after solution of (E-2) for coefficients $\{g_n\}$ and $\{h_n\}$. Equations (E-7) and (E-8) can be solved for $G_x(f)$ and $\mathbf{G}_x(f)$:

$$\begin{bmatrix} A & A^* & B & B^* & A & B^* & A^* & B \\ B & B^* & A & A^* & A & B^* & A^* & B \\ A & B & A & B & A & A & B & B \\ A^* & B^* & A^* & B^* & B^* & B^* & A^* & A^* \end{bmatrix} \begin{bmatrix} G_{x-} \\ G_x \\ G_x \\ G_x^* \end{bmatrix} = \begin{bmatrix} G_{\bar{x}-} \\ G_{\bar{x}} \\ \mathbf{G}_{\bar{x}} \\ \mathbf{G}_{\bar{x}}^* \end{bmatrix}, \quad (E-10)$$

where

$$\begin{aligned} A &\equiv A(f), \quad A_- \equiv A(-f), \\ G_x &\equiv G_x(f), \quad G_{x-} \equiv G_x(-f), \\ \mathbf{G}_x &\equiv \mathbf{G}_x(f), \quad \mathbf{G}_x^* \equiv \mathbf{G}_x^*(f). \end{aligned} \quad (E-11)$$

This requires the inverse of a 4 x 4 complex matrix at each value of frequency f .

Thus an alternative spectral estimation technique is available from the more general prediction model in (E-1). Whether it is worthwhile in terms of stability and resolution is unknown, as it has not been pursued.

LIST OF REFERENCES

1. A. H. Nuttall, Spectral Analysis of a Univariate Process with Bad Data Points, via Maximum Entropy and Linear Predictive Techniques, NUSC Technical Report 5303, 26 March 1976.
2. T. Ulrych and O. Jensen, "Cross-Spectral Analysis Using Maximum Entropy," Geophysics, vol. 39, no. 3, June 1974, pp. 353-354.
3. A. H. Nuttall, Multivariate Linear Predictive Spectral Analysis, Employing Weighted Forward and Backward Averaging: A Generalization of Burg's Algorithm, NUSC Technical Report 5501, 13 October 1976. Program also available in NUSC Technical Document 5419, 19 May 1976.
4. J. F. Ferrie, G. C. Carter, and C. W. Nawrocki, "Availability of Markel's FFT Algorithm," NUSC Technical Memorandum TC-1-73, 15 January 1973.

INITIAL DISTRIBUTION LIST

Addressee	No. of Copies
ASN(R&D)	1
ONR, Code 102-OS, 427, 412-3, 480, 410	5
CNO, OP-090, -095, -098 (981), -902, -96, -983	6
CNM, MAT-00, -03, -03L4, -0302	4
NRL, Underwater Sound Reference Division	2
SUBASE LANT	1
NAVOCEANO, Code 02, 7200	2
NAVELECSYSCOMHQ, Code 03, 051, PME-124	3
NAVSEA, SEA-03C, -032, -06H1, -06H1-3, -09G3, -660, -660E	7
NAVAIRDEVCON	1
NAVWPNSCEN	1
DTNSRDC	1
NAVCOASTSYSLAB	1
CIVENGLAB	1
NAVSURFWPNCEN	1
NELC	1
NUC	1
NAVSEA, SEC-6034	2
NISC	1
NAVPGSCOL	1
APL/UW, Seattle	1
ARL/PENN STATE, State College	1
Center for Naval Analysis (Acquisition Unit)	1
DDC, Alexandria	12
Defense Intelligence Agency	1
Marine Physical Laboratory, Scripps	1
Weapon System Evaluation Group	1
Woods Hole Oceanographic Institution	1